IEEE Access
Multidisciplinary | Rapid Review | Open Access Journal

Received April 17, 2022, accepted May 3, 2022, date of publication May 17, 2022, date of current version May 24, 2022.

Digital Object Identifier 10.1109/ACCESS.2022.3175854

Finite-Time Prescribed Performance Trajectory Tracking Control for Underactuated Autonomous Underwater Vehicles Based on a Tan-Type Barrier Lyapunov Function

HAITAO LIU[1,2], (Member, IEEE), BINGXIN MENG[1], AND XUEHONG TIAN[1,2]
[1]School of Mechanical and Power Engineering, Guangdong Ocean University, Zhanjiang 524088, China
[2]Shenzhen Institute, Guangdong Ocean University, Shenzhen 518120, China

Corresponding author: Bingxin Meng (gdmengbx@126.com)

This work was supported in part by the 2019 "Chong First-Class" Provincial Financial Special Funds Construction Project under Grant 231419019, in part by the Key Project of Department of Education of Guangdong Province under Grant 2021ZDZX1041, and in part by the Science and Technology Planning Project of Zhanjiang City under Grant 2020B01267 and Grant 2021E05012.

ABSTRACT This paper proposed a finite-time prescribed performance control scheme for underactuated autonomous underwater vehicles (AUVs) based on adaptive neural networks and a tan-type barrier Lyapunov function. Even in the presence of output constraints and environmental disturbances, the AUV can also precisely track the desired trajectory in a finite time. By introducing a tan-type barrier Lyapunov Function (TBLF), the singularity problem in process design is solved and all output errors are guaranteed to satisfy the prescribed performance specifications. Dynamic surface control (DSC) and the minimal learning parameter (MLP) are employed to greatly simplify the complexity of the algorithm and enhance the robustness of the control system, respectively. Lyapunov stability analysis proves that the proposed controller guarantees all signals in the closed-loop system to be uniformly ultimately bounded (UUB), and that the tracking errors converge to a small neighborhood near the origin in a finite time. Finally, the simulation results demonstrate the effectiveness and feasibility of the proposed controller.

INDEX TERMS Finite-time stability, trajectory tracking, tan-type barrier Lyapunov function, minimal learning parameter, underactuated autonomous underwater vehicles.

I. INTRODUCTION

In recent years, people have increasingly recognized the indispensability of marine resources to the development of human society. As a result, a wide variety of marine equipment has been vigorously developed. Among them, the research and development of underwater vehicles, especially autonomous underwater vehicles (AUVs), have received much attention, and AUVs have important applications in many fields such as surveillance, rescue, ocean mapping, and inspection of underwater structures[1]. To accomplish the above tasks, AUVs are usually maneuvered in three dimensions in a complex ocean environment. Therefore, the research on trajectory tracking control in 3D space has been a research hotspot in the AUV field.

However, it is difficult to design an AUV trajectory tracking controller due to the obvious dynamic model uncertainties and the time-varying unpredictable disturbances generated by the marine environment. Lapierre *et al.* developed a new type of control law that deals explicitly with vehicle dynamics[2]. Bandara *et al.* proposed a control method using a vehicle fixed frame adaptive controller and an intrinsic nonlinear PID controller for attitude stabilization in complex-shaped low-speed AUV navigation[3]. Furthermore, the disturbances from the environmental external to the AUV should be considered when designing the controller to improve the control performance. In [4], to address the problem that AUVs are subject to model uncertainty and unknown ocean disturbances, the authors construct an iterative neural update law based on the prediction error, which effectively enables the accurate identification of the unknown dynamics of each vehicle. In [5], the trajectory tracking problem with actuator saturation is solved in the presence of parameter uncertainties.

The above work is discussed for fully driven underwater robots. For practical purposes, the design of the control

The associate editor coordinating the review of this manuscript and approving it for publication was Shihong Ding.

system for an underwater underactuated vehicle is very complex and cumbersome because there are only three control inputs to control six degrees of freedom. To overcome the underactuated problem of an AUV, Qiao *et al.* proposed two adaptive fast integral terminal sliding mode control schemes with dual loops [6], and Shojaei *et al.* used the optically guided approach [7]. Seok *et al.* developed additional virtual control inputs to solve the underactuated problem [8]. Sliding model control is an effective control strategy for trajectory tracking. In [9], controllers are designed using the concepts of the terminal sliding model to solve the tracking problem of an underactuated AUV. In [10], the author conquered the quantization effect by introduction the bound of quantization error into the switching term of the SMC. In [11], scholars combine adaptive neural networks and dual closed-loop integral sliding mode control to achieve sliding model control of an underactuated AUV with uncertain dynamics.

Disturbance observers are often used to solve disturbances caused by ocean currents, but due to the powerful approximation ability in controlling nonlinear uncertain systems, adaptive neural networks have received much attention from scholars in recent years. There are many types of neural networks such as the radial basic function neural network (RBFNN) and the convolutional neural network (CNN). In paper [12], an improved neural network model based on the Glasius bio-inspired neural network was proposed and used in AUV trajectory. Paper [13] used neural networks and adaptive techniques to estimate and compensate for uncertainty effects in the AUV control system to achieve 3D trajectory tracking control of underactuated AUVs under the effect of parameter uncertainty and external disturbances. Guo *et al.* introduced a first-order robust exact differentiator, which takes the unknown velocity of the AUV into account, and proposed a nonlinear sliding mode control based on a linear parametric neural network (NSMC-NN) that effectively deals with the unknown dynamics and external environmental disturbances[14]. Elhaki *et al.* used a multilayer neural network and an adaptive robust controller to guarantee the transient performance of the tracking error at a given maximum overshoot and convergence rate, compensating for the structural and nonstructural uncertainties[15]. However, all neural weights of the NN need to be adjusted, causing an unacceptable learning time and complex calculations, which greatly affects the speed of approximation. To avoid this problem, Miao *et al.* adopted the Euclidean norm of the neural weights of the NN to approximate the model uncertainties, which is called the MLP algorithm [16].

In order to enhance the control performance, finite-time convergent and prescribed performance are proposed, which are utilized in many fields except underactuated AUVs. In paper [17], a new finite-time adjustable barrier function is introduced, whose design parameters can be dynamically adjusted in real time as the tracking error changes. Considering the safety of an underwater vehicle, we need to constrain its output to ensure that no accidents occur and the AUV can achieve its target as quickly as possible [18], [19]. In paper [20], a novel high-order sliding mode (HOSM) controller was designed with asymmetric output constraints. In paper [21], a fixed-time controller for a category of nonlinear systems with output constraints was constructed, which can be considered to be an extension of the finite-time control algorithm. Specifically, the output constraint can be satisfied at any time, and the convergence time is independent of the initial conditions and can be predetermined. When the autonomous underwater vehicle is working in a marine environment with coral reefs, ditches or rocks, the AUV cannot move freely without restriction. If we do not want the AUV to collide with the reef and be damaged when passing through some narrow and cramped environments, we should limit its position error as much as possible. On the other hand, when the angle error is too large, the AUV cannot correct the error quickly due to the mechanical system, which will affect the position error. This requires us to further investigate the underwater robot system with output constraints and a quick response strategy.

Inspired by the above-mentioned works, a finite-time convergent prescribed performance control scheme based on the MLP neural network for an underactuated AUV is proposed. The main contributions of this paper are given in the following points.

(1) Compared with [22] and [23], the TBLF and performance function are developed to guarantee the output errors of the systems to be finite-time convergent and limited within a certain region in a finite time.

(2) In contrast to the existing state observers method [24] and RBFNN algorithm [25], the MLP neural network is designed to approximate the model uncertainties and external disturbances, which guarantees that the computational burden of the algorithm can be drastically reduced and improves the system performance. Furthermore, an adaptive law is introduced to estimate the approximation errors.

(3) Dynamic surface control is used to solve the problem of dimensional explosion in the backstepping method. Different from previous works[26, 27], the closed-loop system is finite-time stable and not asymptotically stable. Finite time control can achieve better steady and transient performance and stronger robustness.

The content of this paper is organized as described in the following. Section II presents the relevant preparatory knowledge and some theoretical assumptions. Section III shows the design of the controller. Section IV verifies the effectiveness of this scheme by simulation. Finally, Section V makes some concluding remarks.

A. PRELIMINARY KNOWLEDGE AND PROBLEM FORMULATION

1) MATHEMATICAL MODELING OF THE AUV

In this paper, an underactuated 5-degree-of-freedom AUV subject to environmental disturbances is studied. Fig.1 shows the frame and state of the AUV, and the kinematic and

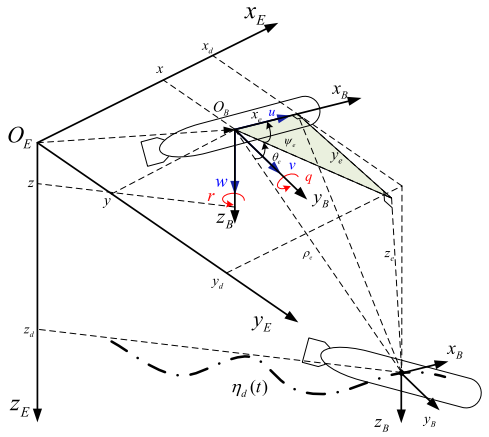

FIGURE 1. Frames and states of underwater vehicles in three dimensions.

dynamical model of this AUV is depicted as follows [28]:

$$\begin{cases} \dot{x} = u\cos\psi\cos\theta - v\sin\psi + w\sin\theta\cos\psi \\ \dot{y} = u\sin\psi\cos\theta + v\cos\psi + w\sin\theta\sin\psi \\ \dot{z} = -u\sin\theta + w\cos\theta \\ \dot{\theta} = q \\ \dot{\psi} = r/\cos\theta \end{cases} \tag{1}$$

$$\begin{cases} \dot{u} = \frac{m_{22}}{m_{11}}vr - \frac{m_{33}}{m_{11}}wq - \frac{d_{11}}{m_{11}}u + \frac{1}{m_{11}}\tau_u + d_u \\ \dot{v} = -\frac{m_{11}}{m_{22}}ur - \frac{d_{22}}{m_{22}}v + d_v \\ \dot{w} = \frac{m_{11}}{m_{33}}uq - \frac{d_{33}}{m_{33}}w + d_w \\ \dot{q} = \frac{(m_{33}-m_{11})}{m_{55}}uw - \frac{d_{55}}{m_{55}}q - \frac{\rho g\overline{GM}_L\sin\theta}{m_{55}} + \frac{1}{m_{55}}\tau_q + d_q \\ \dot{r} = \frac{(m_{11}-m_{22})}{m_{66}}uv - \frac{d_{66}}{m_{66}}r + \frac{1}{m_{66}}\tau_r + d_r \end{cases} \tag{2}$$

where $\eta = (x, y, z, \theta, \psi)^T$ defines the position and orientation; $\upsilon = (u, v, w, q, r)^T$ represents the velocity in each direction;τ_u, $\tau_q$and τ_r represent the control input torque provided by the thrusters and propellers; $d_i(i = u, v, w, q, r)$ stand for the time-varying environmental disturbances caused by wind, waves and ocean currents; $m_{ii}(i = 1, \ldots, 6)$ denote the positive inertia masses of the vehicle; $d_{ii}(i = 1, \ldots, 6)$ are the hydrodynamic coefficients; ρg is the buoyancy of the AUV; and $\overline{GM}_L$ represents the distance between the center of gravity and the floating center[29].

Remark 1: To simplify the controller design in the next section, the dynamics of the rolling motion are ignored in the AUV model. In practice, a recovery force is generated due to the existence of a metacentric height between the center of gravity and the floating center of the AUV. This allows the AUV to stabilize the rolling oscillation by this restoring force at low speed.

Remark 2: In model (2), there is no control input in the second and third equations, which means that the velocities v and w are not controllable during trajectory tracking. This implies that the AUV can only go through three control inputs to accomplish the trajectory tracking mission. Therefore, the AUV is underactuated.

The position and orientation tracking errors between the follower and the target in the inertial reference frame are transformed to the body fixed frame as follows:

$$\begin{cases} x_e = (x - x_d)\cos\theta\cos\psi + (y - y_d)\cos\theta\sin\psi \\ \quad -(z - z_d)\sin\theta \\ y_e = -(x - x_d)\sin\psi + (y - y_d)\cos\psi \\ z_e = (x - x_d)\sin\theta\cos\psi \\ +(y - y_d)\sin\theta\sin\psi + (z - z_d)\cos\theta \end{cases} \tag{3}$$

Differentiating (3) yields the following error dynamics in the body fixed frame:

$$\begin{cases} \dot{x}_e = u - qz_e + ry_e - \dot{x}_d\cos\theta\cos\psi - \dot{y}_d\cos\theta\sin\psi \\ +\dot{z}_d\sin\theta \\ \dot{y}_e = v - r(x_e \\ +\tan\theta z_e) + \dot{x}_d\sin\psi - \dot{y}_d\cos\psi \\ \dot{z}_e = w + qx_e + r\tan\theta y_e - \dot{x}_d\sin\theta\cos y \\ -\dot{y}_d\sin\theta\sin y - \dot{z}_d\cos\theta \end{cases} \tag{4}$$

Then, the tracking errors can be expressed as:

$$\begin{aligned} &\rho_e = \sqrt{x_e^2 + y_e^2 + z_e^2},\ \theta_e = \arctan 2(z_e, \sqrt{x_e^2 + y_e^2}), \\ &\psi_e = \arctan 2(y_e, x_e) \end{aligned} \tag{5}$$

By the above analysis, we can use the following formula to show the position error:

$$\begin{cases} x_e = \rho_e\cos\theta_e\cos\psi_e \\ y_e = \rho_e\cos\theta_e\sin\psi_e \\ z_e = \rho_e\sin\theta_e \end{cases} \tag{6}$$

In order to force the AUV to achieve the desired trajectory, we need to impose some restrictions on the tracking error ρ_e, θ_e and ψ_e. That is, the tracking errorρ_e, θ_e and ψ_e need to satisfy the following time-varying limits:

$$\begin{aligned} -\beta_u(t) < \rho_e < \beta_u(t) \\ -\beta_q(t) < \theta_e < \beta_q(t) \\ -\beta_r(t) < \psi_e < \beta_r(t) \end{aligned} \tag{7}$$

where $-\beta_i(t)$ and $\beta_i(t)$, $i = u, q, r$ are predefined lower and upper bounds for errors ρ_e, θ_e and ψ_e. The boundary functions $\beta_i(t)$, $i = u, q, r$ are taken as:

$$\begin{aligned} \beta_u &= (\beta_{u,0} - \beta_{u,\infty})\exp(-\varpi_u t) + \beta_{u,\infty} \\ \beta_q &= (\beta_{q,0} - \beta_{q,\infty})\exp(-\varpi_q t) + \beta_{q,\infty} \\ \beta_r &= (\beta_{r,0} - \beta_{r,\infty})\exp(-\varpi_r t) + \beta_{r,\infty} \end{aligned} \tag{8}$$

where $\beta_{i,\infty} \leq \beta_{i,0}, (i = u, q, r)$, ϖ_u, ϖ_q and ϖ_r are designed positive constants. $\beta_{u,\infty}$, $\beta_{q,\infty}$ and $\beta_{r,\infty}$ represents the maximum error allowed when the system is stabilized. Eq. (8) is also known as the performance function [30].

B. RBFNN APPROXIMATION

Suppose $f(x) : \mathbb{R}^m \to \mathbb{R}$ is an unknown smooth nonlinear function and it can be approximated over a compact set $\Omega \subseteq \mathbb{R}^m$ with the following RBFNN:

$$f(x) = W^T\phi(x) + \varepsilon \tag{9}$$

$$W = \arg\min_{\hat{w}}\{\sup_{x\in R^m}|f(x) - \hat{W}^T\phi(x)|\} \tag{10}$$

where $W \subseteq R^l$ represents the optimal weight vector, ε is a positive constant representing the approximation error, $\hat{W}$ is the estimation of W^*, $\tilde{W} = W - \hat{W}$, and $\phi(x)$=[$\phi_1(x), \cdots, \phi_l(x)$]^T represents the radial basis function vector, the element of which is chosen as the Gaussian function:

$$\phi_i(x) = \exp(-\frac{||x-\mu_i||^2}{\lambda_i^2}), i = 1, \ldots l \tag{11}$$

where $\mu_i \in \mathbb{R}^m$ and $\lambda_i \in \mathbb{R}$ are the center and spread, respectively, and$|\varepsilon| \le \bar{\varepsilon}$ where $\bar{\varepsilon}$ is an unknown constant.

C. LEMMAS AND ASSUMPTIONS

The following assumptions and theorems will be used in the design.

Assumption 1: The sway velocity and heave velocity of the AUV satisfy $\sup_{t\ge0}|v| < v_m$ and $\sup_{t\ge0}|w| < w_m$, where v_m and w_m are unknown constants.

Remark 3: Assumption 1 always stands due to paper [7]. The assumption is appropriate because the velocities in sway and heave will be damped by the hydrodynamic damping forces.

Assumption 2[22]: The position, speed and acceleration signals of the AUV, i.e., $x_d, y_d, z_d, \dot{x}_d, \dot{y}_d, \dot{z}_d, \ddot{x}_d, \ddot{y}_d, \ddot{z}_d$, have upper and lower bounds.

Assumption 3[22]: The environmental disturbance $d_i(i = u, v, w, q, r,)$ is bounded and satisfies $|d_i| \le \chi_{i,\max}$ with $\chi_{i,\max}$ being an unknown positive constant.

Assumption 4: The pitch angle is bounded such that $|\theta(t)| < \theta_{\max} < \pi/2$.

Remark 4: The pitch angle θ satisfies $|\theta| < \pi/2$ due to the metacentric restoring forces [28] [29].

Lemma 1 [31]: For any $\ell \in \mathbb{R}^+$ and $x \in \mathbb{R}$,the following inequality is established:

$$0 \le |x| - x\tanh(\frac{x}{\ell}) \le \kappa\ell \tag{12}$$

where $\kappa = 0.2785$ satisfies $\kappa = e^{-(\kappa+1)}$.

Lemma 2 [32]: If a nonlinear system $\dot{x} = f(x)$ satisfies $\kappa_1 > 0, \kappa_2 > 0, \varepsilon_v > 0$ and $\alpha \in (0, 1)$ such that

$$\dot{V}(x) \le -\kappa_1 V(x) - \kappa_2 V^\alpha(x) + \varepsilon_v \tag{13}$$

Thus, with the residual set $\Omega_V = \min\left\{\frac{\varepsilon_V}{(1-\Theta)\kappa_1}, (\frac{\varepsilon_V}{(1-\Theta)\kappa_2})^{\frac{1}{\alpha}}\right\}$, the system is practical finite-time stable, where $0 < \Theta < 1$. The settling time is as follows:

$$T(x_0) \le \max\left\{\frac{1}{\kappa_1\Theta(1-\alpha)}\ln(\frac{\kappa_1\Theta V^{1-\alpha}(x_0)+\kappa_2}{\kappa_2}), \frac{1}{\kappa_2\Theta(1-\alpha)}\ln(\frac{\kappa_2\Theta V^{1-\alpha}(x_0)+\kappa_2\Theta}{\kappa_2\Theta})\right\} \tag{14}$$

Lemma 3 [33]: For any $c > 0, a \ge 0, b > 0$, we have $a^c(b-a) \le \frac{1}{1+c}(b^{1+c} - a^{1+c})$.

Lemma 4 [33]: For any $c > 1, a > 0, b \le a$, we have $(a-b)^c \ge b^c - a^c$.

D. TAN-TYPE BARRIER LYAPUNOV FUNCTION

The tan-type barrier Lyapunov function[34] was introduced to constrain the tracking error:

$$V_b = \frac{\beta_b^2}{\pi}\tan(\frac{\pi z^2}{2\beta_b^2}) \tag{15}$$

Remark 5: According to the formulation of TBLF in (15), we can obtain that:

$$\begin{cases}\lim\limits_{z\to0} V_b = 0\\ \lim\limits_{z\to\beta_b} V_b = \infty\end{cases} \tag{16}$$

We can realize that when the initial state $z$satisfies the constraint $\beta_b(0)$, then it will always be maintained. Moreover, if there are no constraints on system states, i.e., $\beta_b \to \infty$, then we can obtain the following equation by using L'Hospital:

$$\lim_{\beta_b\to\infty} V_b = \frac{1}{2}z^2 \tag{17}$$

Therefore, we can directly use the quadratic term to replace the TBLF with no constraints on the dynamic error.

Remark 6: There are many types of barrier Lyapunov functions (BLF) such as the log-type BLF[17, 22] and the tan-type BLF[35]. Eq. (15) should be rewritten to $V_b = \frac{1}{2}\log\frac{\beta_b^2}{\beta_b^2-z^2}$.When$\beta_b \to \infty$, error z is not restricted, and $V_b = 0$. Therefore, the log-type BLF cannot be used as a universal BLF without constraints. Certainly, the tan-type BLF can be used to deal with both constrained and unconstrained situations, but the tan-type BLF is quite complex for underactuated AUV control.

E. CONTROL OBJECTIVE

For a smooth reference trajectory (x_d, y_d, z_d), the control target of this paper is to design TBLF-based control input signals τ_u, τ_q and τ_r to make the AUV follow the target trajectory successfully. In the presence of environmental disturbances, the tracking errors of the AUV achieve the prescribed performance and eventually converge to an arbitrary small neighborhood of the origin. Finally, the adaptive neural network is used to estimate and approximate unknown environmental disturbances from wind, wave and ocean currents.

II. MAIN RESULTS

In this part, a controller based on the TBLF backstepping method with combined DSC and RBFNN techniques is designed for the trajectory tracking problem of an underactuated AUV. The design process is divided into three parts: the design of the virtual control law, the design of the actual control input, and the elimination of environmental disturbances.

A. SURGE MOTION CONTROLLER

The following TBLF candidate should be considered:

$$V_{ue} = \frac{\beta_u^2}{\pi}\tan(\frac{\pi\rho_e^2}{2\beta_u^2}) \tag{18}$$

where β_u is a time-varying function that is a constraint onρ_e.To ensure that V_{ue} is continuous and positively defined,$|\rho_e| \leq \beta_u$ should be set.

Differentiating V_{ue}, we have the following:

$$\dot{V}_{ue} = [2(\rho_e\dot{\rho}_e - \frac{\dot{\beta}_u\rho_e^2}{\beta_u})\csc(\frac{\pi\rho_e^2}{\beta_u^2}) + \frac{2\beta_u\dot{\beta}_u}{\pi}]\tan(\frac{\pi\rho_e^2}{2\beta_u^2}) \tag{19}$$

where $\csc(\bullet) = 1/\sin(\bullet)$.

By differentiating ρ_e in (5), one obtains the following:

$$\begin{aligned}\dot{\rho}_e =\ & u\cos\theta_e\cos\psi_e + v\cos\theta_e\sin\psi_e + w\sin\theta_e \\ & + \cos\theta_e\cos\psi_e(-\dot{x}_d\cos\theta\cos\psi \\ & - \dot{y}_d\cos\theta\sin\psi \\ & + \dot{z}_d\sin\theta) + \cos\theta_e\sin\psi_e(\dot{x}_d\sin\psi - \dot{y}_d\cos\psi) \\ & + \sin\theta_e(-\dot{x}_d\sin\theta\cos\psi - \dot{y}_d\sin\theta\sin\psi - \dot{z}_d\cos\theta)\end{aligned} \tag{20}$$

The following error coordinate transformation can be defined as follows:

$$\begin{aligned}u_e &= u - \alpha_{uc} \\ u_{e1} &= \alpha_{uc} - \alpha_u\end{aligned} \tag{21}$$

The following virtual control lawα_u should be designed:

$$\begin{aligned}\alpha_u =\ & (\cos\theta_e\cos\psi_e)^{-1}(\frac{\dot{\beta}_u}{\beta_u}\rho_e - \frac{\beta_u^2}{2\pi\rho_e} \\ & \times(k_\rho + k_{\rho 1}(\frac{\beta_u^2}{\pi})^{\frac{3}{4}}\tan(\frac{\pi\rho_e^2}{2\beta_u^2})^{-\frac{1}{4}} \\ & + \frac{2\dot{\beta}_u}{\beta_u})\sin(\frac{\pi\rho_e^2}{\beta_u^2}) - v\cos\theta_e\sin\psi_e \\ & - w\sin\theta_e \\ & - \cos\theta_e\cos\psi_e(-\dot{x}_d\cos\theta\cos\psi \\ & - \dot{y}_d\cos\theta\sin\psi \\ & + \dot{z}_d\sin\theta) - \cos\theta_e\sin\psi_e(\dot{x}_d\sin\psi - \dot{y}_d\cos\psi) \\ & - \sin\theta_e \\ & \times(-\dot{x}_d\sin\theta\cos\psi - \dot{y}_d\sin \\ & \times\theta\sin\psi - \dot{z}_d\cos\theta))\end{aligned} \tag{22}$$

where the design parameters $k_\rho > 0, k_{\rho 1} > 0$.

According to (16-18), $\dot{V}_{ue}$ is simplified as

$$\begin{aligned}\dot{V}_{ue} =\ & -k_\rho\frac{\beta_u^2}{\pi}\tan(\frac{\pi\rho_e^2}{2\beta_u^2}) - k_{\rho 1}(\frac{\beta_u^2}{\pi}\tan(\frac{\pi\rho_e^2}{2\beta_u^2}))^{\frac{3}{4}} \\ & + 2u_e\rho_e\cos\theta_e\cos\psi_e\sec^2(\frac{\pi\rho_e^2}{2\beta_u^2}) \\ & + 2u_{e1}\rho_e\cos\theta_e\cos\psi_e\sec^2(\frac{\pi\rho_e^2}{2\beta_u^2})\end{aligned} \tag{23}$$

A first-order filter is used to reduce the computational complexity of the traditional backstepping method:

$$\kappa_u\dot{\alpha}_{uc} + \alpha_{uc} = \alpha_{mu},\ \alpha_{uc}(0) = \alpha_{mu}(0) \tag{24}$$

with $\alpha_{mu} = \alpha_u + 2\kappa_u\rho_e\cos\psi_e\cos\theta_e\sec^2(\frac{\pi\rho_e^2}{2\beta_u^2})$, where α_u is the filtered virtual control law and $\kappa_u > 0$ is the designed time constant. The derivative of u_{e1} is as follows:

$$\dot{u}_{e1} = -\kappa_u^{-1}u_{e1} - 2\rho_e\cos\theta_e\cos\psi_e\sec^2(\frac{\pi\rho_e^2}{2\beta_u^2}) - B_u(\bullet) \tag{25}$$

where $\dot{\alpha}_u B_u(\bullet)$ with $B_u(\eta, \dot{\eta}, \ddot{\eta}, v, w, \beta_u, \dot{\beta}_u, \ddot{\beta}_u, \rho_e, u_e, u_{e1})$ being continuous functions.

The quadratic Lyapunov function below should be chosen since there is no restriction on u_e and u_{e1}:

$$\begin{aligned}V_{ue2} &= V_{ue} + \frac{1}{2}u_e^2 + \frac{1}{2}u_{e1}^2 \\ &= \frac{\beta_u^2}{\pi}\tan(\frac{\pi\rho_e^2}{2\beta_u^2}) + \frac{1}{2}u_e^2 + \frac{1}{2}u_{e1}^2\end{aligned} \tag{26}$$

The time derivative of V_{ue2} is given by:

$$\begin{aligned}\dot{V}_{ue2} &= \dot{V}_{ue} + u_e\dot{u}_e + u_{e1}\dot{u}_{e1} \\ &= -k_\rho\frac{\beta_u^2}{\pi}\tan(\frac{\pi\rho_e^2}{2\beta_u^2}) - k_{\rho 1}(\frac{\beta_u^2}{\pi}\tan(\frac{\pi\rho_e^2}{2\beta_u^2}))^{\frac{3}{4}} \\ & + 2\rho_e u_e\cos\psi_e\cos\theta_e\sec^2(\frac{\rho_e^2\pi}{2\beta_u^2}) \\ & + 2\rho_e u_{e1}\cos\psi_e\cos\theta_e\sec^2(\frac{\rho_e^2\pi}{2\beta_u^2}) + u_e(\dot{u} - \dot{\alpha}_{uc}) \\ & + u_{e1}(-\kappa_u^{-1}u_{e1} - 2\rho_e\cos\theta_e\cos\psi_e\sec^2(\frac{\pi\rho_e^2}{2\beta_u^2}) \\ & - B_u(\cdot)) = -k_\rho\frac{\beta_u^2}{\pi}\tan(\frac{\pi\rho_e^2}{2\beta_u^2}) - k_{\rho 1}(\frac{\beta_u^2}{\pi}\tan(\frac{\pi\rho_e^2}{2\beta_u^2}))^{\frac{3}{4}} \\ & + 2u_e\rho_e\cos\theta_e\cos\psi_e\sec^2(\frac{\pi\rho_e^2}{2\beta_u^2}) \\ & + u_e(\frac{m_{22}}{m_{11}}vr - \frac{m_{33}}{m_{11}}wq - \frac{d_{11}}{m_{11}}u + \frac{1}{m_{11}}\tau_u \\ & + d_u - \dot{\alpha}_{uc}) - \kappa_u^{-1}u_{e1}^2 - u_{e1}B_u(\bullet)\end{aligned} \tag{27}$$

Defining $\hat{\lambda}_u = ||\hat{W}_u||^2$, $\partial_u = \frac{\phi_u^2(x_u)}{2b_u}$ [16], the surge control law is designed as:

$$\begin{aligned}\tau_u =\ & m_{11}(-k_u u_e - k_{u1}u_e^{\frac{1}{2}} - \kappa_{u1}u_{e1}^{\frac{3}{2}}u_e^{-1} - \frac{m_{22}}{m_{11}}vr + \frac{m_{33}}{m_{11}}wq \\ & + \frac{d_{11}}{m_{11}}u + \dot{\alpha}_{uc} - 2\rho_e\cos\theta_e\cos\psi_e\sec^2(\frac{\pi\rho_e^2}{2\beta_u^2}) \\ & - \hat{\lambda}_u\partial_u u_e - \tanh(\frac{u_e}{\ell_u})\hat{h}_u)\end{aligned} \tag{28}$$

$$\dot{\hat{\lambda}}_u = \partial_u u_e^2 - k_{\lambda u}\hat{\lambda}_u - k_{\lambda u1}\hat{\lambda}_u^{\frac{1}{2}} \tag{29}$$

$$\dot{\hat{h}}_u = u_e\tanh(\frac{u_e}{\ell_u}) - k_{\hbar u}\hat{h}_u - k_{\hbar u1}\hat{h}_u^{\frac{1}{2}} \tag{30}$$

where $x_u = [u, \dot{\alpha}_{uc}]^T$, $b_u, k_{\lambda u}, k_{\hbar u}, k_{\lambda u1}, k_{\hbar u1}$ are positive design parameters.

B. PITCH MOTION CONTROLLER

The following TBLF candidate should be considered:

$$V_{qe} = \frac{\beta_q^2}{\pi}\tan(\frac{\pi\theta_e^2}{2\beta_q^2}) \tag{31}$$

where β_q is a time-varying function that is a constraint on θ_e.

Differentiating V_{qe}, we have the following:

$$\begin{aligned}\dot{V}_{qe} = [&2(\theta_e\dot{\theta}_e \\ &-\frac{\dot{\beta}_q\theta_e^2}{\beta_q})\csc(\frac{\pi\theta_e^2}{\beta_q^2}) + \frac{2\beta_q\dot{\beta}_q}{\pi}]\tan(\frac{\pi\theta_e^2}{2\beta_q^2})\end{aligned} \tag{32}$$

By differentiating θ_e in (5), one obtains the following:

$$\begin{aligned}\dot{\theta}_e = &q\cos\psi_e + r\tan\theta\sin\psi_e + \cos\theta_e(w - \dot{x}_d\sin\theta\cos\psi \\ &-\dot{y}_d\sin\theta\sin\psi - \dot{z}_d\cos\theta)/\rho_e - \sin\theta_e\cos\psi_e(u \\ &-\dot{x}_d\cos\theta\cos\psi - \dot{y}_d\cos\theta\sin\phi + \dot{z}_d\sin\theta)/\rho_e \\ &-\sin\theta_e\sin\psi_e(v + \dot{x}_d\sin\psi - \dot{y}_d\cos\psi)/\rho_e\end{aligned} \tag{33}$$

The following error coordinate transformation should be defined:

$$\begin{aligned}q_e &= q - \alpha_{qc} \\ q_{e1} &= \alpha_{qc} - \alpha_q\end{aligned} \tag{34}$$

The following virtual control lawα_q should be defined:

$$\begin{aligned}\alpha_q = &(\cos\psi_e)^{-1}(\frac{\dot{\beta}_q}{\beta_q}\theta_e - \frac{\beta_q^2}{2\pi\theta_e}(k_\theta \\ &+k_{\theta1}(\frac{\beta_q^2}{\pi})^{\frac{3}{4}}\tan(\frac{\pi\theta_e^2}{2\beta_q^2})^{-\frac{1}{4}} \\ &+\frac{2\dot{\beta}_q}{\beta_q})\sin(\frac{\pi\theta_e^2}{\beta_q^2}) - r\tan\theta\sin\psi_e \\ &-\cos\theta_e(w - \dot{x}_d\sin\theta\cos\psi \\ &-\dot{y}_d\sin\theta\sin\psi - \dot{z}_d\cos\theta)/\rho_e + \sin\theta_e\cos\psi_e(u \\ &-\dot{x}_d\cos\theta\cos\psi - \dot{y}_d\cos\theta\sin\phi + \dot{z}_d\sin\theta)/\rho_e \\ &+\sin\theta_e\sin\psi_e(v + \dot{x}_d\sin\psi - \dot{y}_d\cos\psi)/\rho_e)\end{aligned} \tag{35}$$

where the design parameters $k_\theta > 0, k_{\theta1} > 0$. Combing (32) and (33), one can obtain the following:

$$\begin{aligned}\dot{V}_{qe} = &-k_\theta\frac{\beta_q^2}{\pi}\tan(\frac{\pi\theta_e^2}{2\beta_q^2}) - k_{\theta1}(\frac{\beta_q^2}{\pi}\tan(\frac{\pi\theta_e^2}{2\beta_q^2}))^{\frac{3}{4}} \\ &+2q_e\theta_e\cos\psi_e\sec^2(\frac{\pi\theta_e^2}{2\beta_q^2}) \\ &+2q_{e1}\theta_e\cos\psi_e\sec^2(\frac{\pi\theta_e^2}{2\beta_q^2})\end{aligned} \tag{36}$$

The virtual control law is filtered using a first-order filter below:

$$\kappa_q\dot{\alpha}_{qc} + \alpha_{qc} = \alpha_{mq},\ \alpha_{qc}(0) = \alpha_{mq}(0) \tag{37}$$

with $\alpha_{mq} = \alpha_u + 2\kappa_q\theta_e\cos\psi_e\sec^2(\frac{\pi\theta_e^2}{2\beta_q^2})$, where α_q is the filtered virtual control law and $\kappa_q > 0$ is the designed time constant. The derivative of q_{e1} is:

$$\dot{q}_{e1} = -\kappa_q^{-1}q_{e1} - 2\theta_e\cos\psi_e\sec^2(\frac{\pi\theta_e^2}{2\beta_q^2}) - B_q(\cdot) \tag{38}$$

where $\dot{\alpha}_qB_q(\bullet)$ with $B_q(\eta, \dot{\eta}, \ddot{\eta}, u, v, w, r, \beta_q, \dot{\beta}_q, \ddot{\beta}_q, \theta_e, q_e, q_{e1})$ being continuous functions.

Then, the QLF should be chosen as follows:

$$V_{qe2} = V_{qe} + \frac{1}{2}q_e^2 + \frac{1}{2}q_{e1}^2 = \frac{\beta_q^2}{\pi}\tan(\frac{\pi\theta_e^2}{2\beta_q^2}) + \frac{1}{2}q_e^2 + \frac{1}{2}q_{e1}^2 \tag{39}$$

By differentiating V_{qe2}, one obtains the following:

$$\begin{aligned}\dot{V}_{qe2} &= \dot{V}_{qe} + q_e\dot{q}_e + q_{e1}\dot{q}_{e1} \\ &= -k_\theta\frac{\beta_q^2}{\pi}\tan(\frac{\pi\theta_e^2}{2\beta_q^2}) - k_{\theta1}(\frac{\beta_q^2}{\pi}\tan(\frac{\pi\theta_e^2}{2\beta_q^2}))^{\frac{3}{4}} \\ &\quad+2q_e\theta_e\cos\psi_e\sec^2(\frac{\pi\theta_e^2}{2\beta_q^2}) \\ &\quad+2q_{e1}\theta_e\cos\psi_e\sec^2(\frac{\pi\theta_e^2}{2\beta_q^2}) + q_e(\dot{q} - \dot{\alpha}_{qc}) \\ &\quad+q_{e1}(-\kappa_q^{-1}q_{e1} + 2\theta_e\cos\psi_e\sec^2(\frac{\pi\theta_e^2}{2\beta_q^2}) - B_q(\bullet)) \\ &= -k_\theta\frac{\beta_q^2}{\pi}\tan(\frac{\pi\theta_e^2}{2\beta_q^2}) - k_{\theta1}(\frac{\beta_q^2}{\pi}\tan(\frac{\pi\theta_e^2}{2\beta_q^2}))^{\frac{3}{4}} \\ &\quad+2q_e\theta_e\cos\psi_e\sec^2(\frac{\pi\theta_e^2}{2\beta_q^2}) + q_e(\frac{(m_{33} - m_{11})}{m_{55}}uw \\ &\quad-\frac{d_{55}}{m_{55}}q - \frac{\rho g\overline{GM}_L\sin\theta}{m_{55}} + \frac{1}{m_{55}}\tau_q + d_q \\ &\quad-\dot{\alpha}_{qc}) \\ &\quad-\kappa_q^{-1}q_{e1}^2 - q_{e1}B_q(\bullet)\end{aligned} \tag{40}$$

Defining $\hat{\lambda}_q = ||\hat{W}_q||^2$, $\partial_q = \frac{\phi_q^2(x_q)}{2b_q}$, the pitch torque can be designed as follows:

$$\begin{aligned}\tau_q = m_{55}(&-k_qq_e - k_{q1}q_e^{\frac{1}{2}} - \kappa_{q1}q_{e1}^{\frac{3}{2}}q_e^{-1} - \frac{(m_{33} - m_{11})}{m_{55}}uw \\ &-2\theta_e\cos\psi_e\sec^2(\frac{\pi\theta_e^2}{2\beta_q^2}) + \dot{\alpha}_{qc} + \frac{d_{55}}{m_{55}}q \\ &+\frac{\rho g\overline{GM}_L\sin\theta}{m_{55}} - \hat{\lambda}_q\partial_qq_e - \tanh(\frac{q_e}{\ell_q})\hat{\hbar}_q)\end{aligned} \tag{41}$$

$$\dot{\hat{\lambda}}_q = \partial_qq_e^2 - k_{\lambda q}\hat{\lambda}_q - k_{\lambda q1}\hat{\lambda}_q^{\frac{1}{2}} \tag{42}$$

$$\dot{\hat{\hbar}}_q = q_e\tanh(\frac{q_e}{\ell_q}) - k_{\hbar q}\hat{\lambda}_q - k_{\hbar q1}\hat{\hbar}_q^{\frac{1}{2}} \tag{43}$$

where $x_q = [q, \dot{\alpha}_{qc}]^T, b_q, k_{\lambda q}, k_{\hbar q}, k_{\lambda q1}, k_{\hbar q1}$ are positive design parameters.

C. YAW MOTION CONTROLLER

The following TBLF candidate should be considered:

$$V_{re} = \frac{\beta_r^2}{\pi}\tan(\frac{\pi\psi_e^2}{2\beta_r^2}) \tag{44}$$

By differentiating V_{re}, we have the following;

$$\dot{V}_{re} = [2(\psi_e\dot{\psi}_e - \frac{\dot{\beta}_r\psi_e^2}{\beta_r})\csc(\frac{\pi\psi_e^2}{\beta_r^2}) + \frac{2\beta_r\dot{\beta}_r}{\pi}]\tan(\frac{\pi\psi_e^2}{2\beta_r^2}) \tag{45}$$

By differentiating ψ_e in (5), we obtain the following:

$$\begin{aligned}\dot{\psi}_e =& -r(1+\tan\theta\tan\theta_e\cos\psi_e) + q\tan\theta_e\sin\psi_e \\ &+(v+\dot{x}_d\sin\psi - \dot{y}_d\cos\psi)\cos\psi_e/\rho_e\cos\theta_e \\ &-(u-\dot{x}_d\cos\theta\cos\psi - \dot{y}_d\cos\theta\sin\psi \\ &+\dot{z}_d\sin\theta)\sin\psi_e/\rho_e\cos\theta_e\end{aligned} \tag{46}$$

The following error coordinate transformation can be defined as follows:

$$\begin{aligned}r_e &= r - \alpha_{rc} \\ r_{e1} &= \alpha_{rc} - \alpha_r\end{aligned} \tag{47}$$

The following virtual control law$\alpha_r$can be defined as follows:

$$\begin{aligned}\alpha_r =& (\tan\theta\cos\psi_e\tan\theta_e+1)^{-1}(\frac{\beta_r^2}{2\pi\psi_e}(k_\psi \\ &+k_{\psi 1}(\frac{\beta_r^2}{\pi})^{\frac{3}{4}}\tan(\frac{\pi\psi_e^2}{2\beta_r^2})^{-\frac{1}{4}} + \frac{2\dot{\beta}_r}{\beta_r})\sin(\frac{\pi\psi_e^2}{\beta_r^2}) \\ &-\frac{\dot{\beta}_r}{\beta_r}\psi_e + q\tan\theta_e\sin\psi_e - (v+\dot{x}_d\sin\psi \\ &-\dot{y}_d\cos\psi)\cos\psi_e/\rho_e\cos\theta_e - (u-\dot{x}_d\cos\theta\cos\psi \\ &-\dot{y}_d\cos\theta\sin\psi + \dot{z}_d\sin\theta)\sin\psi_e/\rho_e\cos\theta_e)\end{aligned} \tag{48}$$

where the design parameters $k_\psi > 0, k_{\psi 1} > 0$. The simplified $\dot{V}_{re}$ can be obtained as follows:

$$\begin{aligned}\dot{V}_{re} =& -k_\psi\frac{\beta_r^2}{\pi}\tan(\frac{\pi\psi_e^2}{2\beta_r^2}) - k_{\psi 1}(\frac{\beta_r^2}{\pi}\tan(\frac{\pi\psi_e^2}{2\beta_r^2}))^{\frac{3}{4}} \\ &+2r_e\psi_e(\tan\theta\cos\psi_e\tan\theta_e+1)\sec^2(\frac{\pi\theta_e^2}{2\beta_r^2}) \\ &+2r_{e1}\psi_e(\tan\theta\cos\psi_e\tan\theta_e+1)\sec^2(\frac{\pi\theta_e^2}{2\beta_r^2})\end{aligned} \tag{49}$$

The virtual control law is filtered using a first-order filter below:

$$\kappa_r\dot{\alpha}_c + \alpha_{rc} = \alpha_{mr},\ \alpha_{rc}(0) = \alpha_{mr}(0) \tag{50}$$

with $\alpha_{mr} = \alpha_r + 2\kappa_r\psi_e(1+\tan\theta\tan\theta_e\cos\psi_e)\sec^2(\frac{\pi\theta_e^2}{2\beta_r^2})$, where α_r is the filtered virtual control law and $\kappa_r > 0$ is the designed time constant. The derivative of r_{e1} is as follows:

$$\begin{aligned}\dot{r}_{e1} =& -\kappa_r^{-1}r_{e1} - 2\psi_e(1+\tan\theta\tan\theta_e\cos\psi_e)\sec^2(\frac{\pi\theta_e^2}{2\beta_r^2}) \\ &-B_r(\cdot)\end{aligned} \tag{51}$$

where $\dot{\alpha}_r B_r(\cdot)$ with $B_r(\eta, \dot{\eta}, \ddot{\eta}, u, v, q, \beta_r, \dot{\beta}_r, \ddot{\beta}_r, \psi_e, r_e, r_{e1})$ being continuous functions.

Then, the QLF is considered as follows:

$$V_{re2} = V_{re} + \frac{1}{2}r_e^2 + \frac{1}{2}r_{e1}^2 = \frac{\beta_r^2}{\pi}\tan(\frac{\pi\psi_e^2}{2\beta_r^2}) + \frac{1}{2}r_e^2 + \frac{1}{2}r_{e1}^2 \tag{52}$$

By differentiating V_{re2}, one obtains the following:

$$\begin{aligned}\dot{V}_{re2} =& -k_\psi\frac{\beta_r^2}{\pi}\tan(\frac{\pi\psi_e^2}{2\beta_r^2}) - k_{\psi 1}(\frac{\beta_r^2}{\pi}\tan(\frac{\pi\psi_e^2}{2\beta_r^2}))^{\frac{3}{4}} \\ &+2r_e\psi_e(\tan\theta\cos\psi_e\tan\theta_e+1)\sec^2(\frac{\pi\theta_e^2}{2\beta_r^2}) \\ &+2r_{e1}\psi_e(\tan\theta\cos\psi_e\tan\theta_e+1)\sec^2(\frac{\pi\theta_e^2}{2\beta_r^2}) \\ &+r_e(\dot{r}-\dot{\alpha}_{rc}) + r_{e1}(-\kappa_r^{-1}r_{e1} \\ &-2\psi_e(\tan\theta\cos\psi_e\tan\theta_e+1)\sec^2(\frac{\pi\theta_e^2}{2\beta_r^2}) - B_r(\cdot)) \\ =& -k_\psi\frac{\beta_r^2}{\pi}\tan(\frac{\pi\psi_e^2}{2\beta_r^2}) - k_{\psi 1}(\frac{\beta_r^2}{\pi}\tan(\frac{\pi\psi_e^2}{2\beta_r^2}))^{\frac{3}{4}} \\ &+2r_e\psi_e(1+\tan\theta\tan\theta_e\cos\psi_e)\sec^2(\frac{\pi\theta_e^2}{2\beta_r^2}) \\ &+r_e(\frac{(m_{11}-m_{22})}{m_{66}}uv - \frac{d_{66}}{m_{66}}r + \frac{1}{m_{66}}\tau_r + d_r - \dot{\alpha}_{rc}) \\ &-\kappa_r^{-1}r_{e1}^2 - r_{e1}B_r(\cdot)\end{aligned} \tag{53}$$

Defining $\hat{\bar{\lambda}}_r = ||\hat{W}_r||^2$, $\partial_r = \frac{\phi_r^2(x_r)}{2b_r}$, the following yaw controller is designed:

$$\begin{aligned}\tau_r =& m_{66}(-k_r r_e - k_{r1}r_e^{\frac{1}{2}} - \kappa_{r1}r_{e1}^{\frac{3}{2}}r_e^{-1} \\ &-2\psi_e(1+\tan\theta\tan\theta_e\cos\psi_e)\sec^2(\frac{\pi r_e^2}{2\beta_r^2}) \\ &+\dot{\alpha}_{rc} - \frac{m_{11}-m_{22}}{m_{66}}uv + \frac{d_{66}}{m_{66}}r - \hat{\bar{\lambda}}_r\partial_r r_e \\ &-\tanh(\frac{r_e}{\ell_r})\hat{\bar{h}}_r)\end{aligned} \tag{54}$$

$$\dot{\hat{\bar{\lambda}}}_r = \partial_r r_e^2 - k_{\lambda r}\hat{\bar{\lambda}}_r - k_{\lambda r1}\hat{\bar{\lambda}}_r^{\frac{1}{2}} \tag{55}$$

$$\dot{\hat{\bar{h}}}_r = r_e\tanh(\frac{r_e}{\ell_r}) - k_{\eta r}\hat{\bar{h}}_r - k_{\eta r1}\hat{\bar{h}}_r^{\frac{1}{2}} \tag{56}$$

where $x_r = [r, \dot{\alpha}_{rc}]^T, b_r, k_{\lambda r}, k_{\eta r}, k_{\lambda r1}, k_{\eta r1}$ are positive design parameters.

Fig.2 shows a block diagram of the proposed control system. In the next part, the stability analysis of the control system is presented.

D. LYAPUNOV STABILITY ANALYSIS

Theorem 1: For the trajectory tracking problem of an underactuated AUV with models (1) and (2), if the initial errors limited in the bound and all assumptions are valid, then it is guaranteed that all closed-loop system signals in controllers (22), (24), (28), (29), (30), (35), (37), (41), (42), (43), (48), (50), (54), (55) and (56) are uniformly ultimately bounded. The system outputs can reach the prescribed performance throughout the process and eventually converge

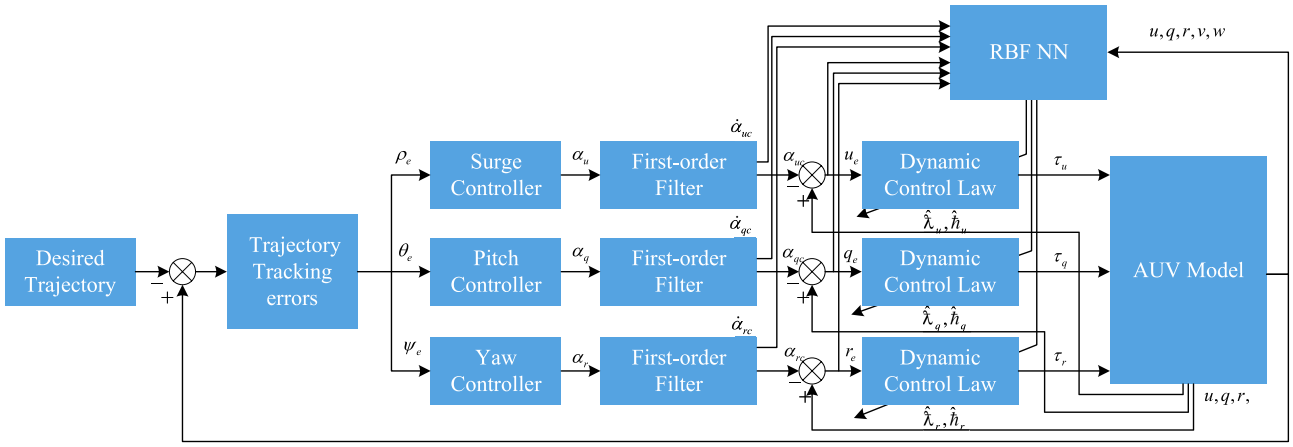

FIGURE 2. Block diagram of the proposed target tracking control system.

to a small area near zero in a finite time whose radius is adjustable by control parameters.

Proof: By constructing the following Lyapunov function:

$$V = \frac{\beta_u^2}{\pi}\tan(\frac{\pi\rho_e^2}{2\beta_u^2}) + \frac{\beta_q^2}{\pi}\tan(\frac{\pi\theta_e^2}{2\beta_q^2}) + \frac{\beta_r^2}{\pi}\tan(\frac{\pi\psi_e^2}{2\beta_r^2}) + \frac{1}{2}u_e^2 + \frac{1}{2}q_e^2 + \frac{1}{2}r_e^2 + \frac{1}{2}u_{e1}^2 + \frac{1}{2}q_{e1}^2 + \frac{1}{2}r_{e1}^2 + \frac{1}{2}\tilde{\lambda}_u^2 + \frac{1}{2}\tilde{\lambda}_q^2 + \frac{1}{2}\tilde{\lambda}_r^2 + \frac{1}{2}\tilde{h}_u^2 + \frac{1}{2}\tilde{h}_q^2 + \frac{1}{2}\tilde{h}_r^2 \quad (57)$$

we can obtain:

$$\begin{aligned}\dot{V} = &-k_\rho\frac{\beta_u^2}{\pi}\tan(\frac{\pi\rho_e^2}{2\beta_u^2}) - k_{\rho1}(\frac{\beta_u^2}{\pi}\tan(\frac{\pi\rho_e^2}{2\beta_u^2}))^{\frac{3}{4}}\\ &-k_\theta\frac{\beta_q^2}{\pi}\tan(\frac{\pi\theta_e^2}{2\beta_q^2}) - k_{\theta1}(\frac{\beta_q^2}{\pi}\tan(\frac{\pi\theta_e^2}{2\beta_q^2}))^{\frac{3}{4}}\\ &-k_\psi\frac{\beta_r^2}{\pi}\tan(\frac{\pi\psi_e^2}{2\beta_r^2}) - k_{\psi1}(\frac{\beta_r^2}{\pi}\tan(\frac{\pi\psi_e^2}{2\beta_r^2}))^{\frac{3}{4}}\\ &-k_u u_e^2 - k_{u1}u_e^{\frac{3}{2}} - k_q q_e^2 - k_{q1}q_e^{\frac{3}{2}} - k_r r_e^2 - k_{r1}u_r^{\frac{3}{2}}\\ &-\kappa_u^{-1}u_{e1}^2 - \kappa_{u1}u_{e1}^{\frac{3}{2}} - \kappa_q^{-1}q_{e1}^2 - \kappa_{q1}q_{e1}^{\frac{3}{2}} - \kappa_r^{-1}r_{e1}^2\\ &-\kappa_{r1}r_{e1}^{\frac{3}{2}} - u_{e1}B_u(\cdot) - q_{e1}B_q(\cdot) - r_{e1}B_r(\cdot)\\ &-\hat{\tilde{\lambda}}_u\partial_u u_e^2 - \hat{\tilde{\lambda}}_u\partial_u u_e^2 - \hat{\tilde{\lambda}}_r\partial_r r_e^2 - \lambda_u\partial_u u_e^2\\ &-\lambda_q\partial_q q_e^2 - \lambda_r\partial_r r_e^2 + u_e\hbar_u + q_e\hbar_q + r_e\hbar_r\\ &-u_e\tanh(\frac{u_e}{\ell_u})\hat{h}_u - q_e\tanh(\frac{q_e}{\ell_q})\hat{h}_q - r_e\tanh(\frac{r_e}{\ell_r})\hat{h}_r\\ &-\tilde{\lambda}_u\dot{\tilde{\lambda}}_u - \tilde{\lambda}_q\dot{\tilde{\lambda}}_q - \tilde{\lambda}_r\dot{\tilde{\lambda}}_r - \tilde{h}_u\dot{\tilde{h}}_u - \tilde{h}_q\dot{\tilde{h}}_q - \tilde{h}_r\dot{\tilde{h}}_r\\ &+\frac{b_u}{2} + \frac{b_q}{2} + \frac{b_r}{2}\\ \le &-k_\rho\frac{\beta_u^2}{\pi}\tan(\frac{\pi\rho_e^2}{2\beta_u^2}) - k_{\rho1}(\frac{\beta_u^2}{\pi}\tan(\frac{\pi\rho_e^2}{2\beta_u^2}))^{\frac{3}{4}}\\ &-k_\theta\frac{\beta_q^2}{\pi}\tan(\frac{\pi\theta_e^2}{2\beta_q^2}) - k_{\theta1}(\frac{\beta_q^2}{\pi}\tan(\frac{\pi\theta_e^2}{2\beta_q^2}))^{\frac{3}{4}}\\ &-k_\psi\frac{\beta_r^2}{\pi}\tan(\frac{\pi\psi_e^2}{2\beta_r^2}) - k_{\psi1}(\frac{\beta_r^2}{\pi}\tan(\frac{\pi\psi_e^2}{2\beta_r^2}))^{\frac{3}{4}}\\ &-k_u u_e^2 - k_{u1}u_e^{\frac{3}{2}} - k_q q_e^2 - k_{q1}q_e^{\frac{3}{2}} - k_r r_e^2 - k_{r1}u_r^{\frac{3}{2}}\\ &-\kappa_u^{-1}u_{e1}^2 - \kappa_{u1}u_{e1}^{\frac{3}{2}} - \kappa_q^{-1}q_{e1}^2 - \kappa_{q1}q_{e1}^{\frac{3}{2}} - \kappa_r^{-1}r_{e1}^2\\ &-\kappa_{r1}r_{e1}^{\frac{3}{2}} - u_{e1}B_u(\cdot) - q_{e1}B_q(\cdot) - r_{e1}B_r(\cdot)\\ &+k_{\lambda u}\tilde{\lambda}_u\hat{\tilde{\lambda}}_u + k_{\lambda u1}\tilde{\lambda}_u\hat{\tilde{\lambda}}_u^{\frac{1}{2}} + k_{\lambda q}\tilde{\lambda}_q\hat{\tilde{\lambda}}_q + k_{\lambda q1}\tilde{\lambda}_q\hat{\tilde{\lambda}}_q^{\frac{1}{2}}\\ &+k_{\lambda r}\tilde{\lambda}_r\hat{\tilde{\lambda}}_r + k_{\lambda r1}\tilde{\lambda}_r\hat{\tilde{\lambda}}_r^{\frac{1}{2}} + k_{\eta u}\tilde{h}\hat{\tilde{h}}_u + k_{\eta u1}\tilde{h}\hat{\tilde{h}}_u^{\frac{1}{2}}\\ &+k_{\eta q}\tilde{h}\hat{\tilde{h}}_q + k_{\eta q1}\tilde{h}\hat{\tilde{h}}_q^{\frac{1}{2}} + k_{\eta r}\tilde{h}\hat{\tilde{h}}_r + k_{\eta r1}\tilde{h}\hat{\tilde{h}}_r^{\frac{1}{2}}\\ &+\kappa\ell_u\hbar_u + \kappa\ell_q\hbar_q + \kappa\ell_r\hbar_r + \frac{b_u}{2} + \frac{b_q}{2} + \frac{b_r}{2} \quad (59)\end{aligned}$$

The unknown disturbances d_i could be estimated by RBFs such as $d_i = W_i\phi_i(x_i) + \varepsilon_i, i = u, q, r$.

Thus, Eq. (58) is simplified as:

$$\dot{V} \le -k_\rho\frac{\beta_u^2}{\pi}\tan(\frac{\pi\rho_e^2}{2\beta_u^2}) - k_{\rho1}(\frac{\beta_u^2}{\pi}\tan(\frac{\pi\rho_e^2}{2\beta_u^2}))^{\frac{3}{4}}$$

Since $\hat{\tilde{\lambda}}_i > 0$ and $-\lambda_i > 0$, using Lemma 3 and Lemma 4, one obtains:

$$\begin{aligned}\tilde{\lambda}_i\hat{\tilde{\lambda}}_i^z &= \hat{\tilde{\lambda}}_i^z(-\lambda_i - \hat{\tilde{\lambda}}_i)\\ &\le \frac{1}{1+z}(-\lambda_i^{1+z} - (-\lambda_i - \tilde{\lambda}_i)^{1+z})\\ &\le \frac{1}{1+z}(2^z-\lambda_i^{1+z} - \tilde{\lambda}_i^{1+z})\end{aligned} \tag{60}$$

Combining the inequality (60) and Young's inequality, one obtains:

$$\begin{aligned}\dot{V} \le & -k_\rho\frac{\beta_u^2}{\pi}\tan(\frac{\pi\rho_e^2}{2\beta_u^2}) - k_{\rho1}(\frac{\beta_u^2}{\pi}\tan(\frac{\pi\rho_e^2}{2\beta_u^2}))^{\frac{3}{4}}\\ & - k_\theta\frac{\beta_q^2}{\pi}\tan(\frac{\pi\theta_e^2}{2\beta_q^2}) - k_{\theta1}(\frac{\beta_q^2}{\pi}\tan(\frac{\pi\theta_e^2}{2\beta_q^2}))^{\frac{3}{4}}\\ & - k_\psi\frac{\beta_r^2}{\pi}\tan(\frac{\pi\psi_e^2}{2\beta_r^2}) - k_{\psi1}(\frac{\beta_r^2}{\pi}\tan(\frac{\pi\psi_e^2}{2\beta_r^2}))^{\frac{3}{4}}\\ & - k_u u_e^2 - k_{u1}u_e^{\frac{3}{2}} - k_q q_e^2 - k_{q1}q_e^{\frac{3}{2}} - k_r r_e^2 - k_{r1}u_r^{\frac{3}{2}}\\ & - (\kappa_u^{-1} - \frac{1}{2})u_{e1}^2 - \kappa_{u1}u_{e1}^{\frac{3}{2}} - (\kappa_q^{-1} - \frac{1}{2})q_{e1}^2 - \kappa_{q1}q_{e1}^{\frac{3}{2}}\\ & - (\kappa_r^{-1} - \frac{1}{2})r_{e1}^2 - \kappa_{r1}r_{e1}^{\frac{3}{2}} + \frac{1}{2}B_u^2 + \frac{1}{2}B_q^2\\ & + \frac{1}{2}B_r^2 - \frac{1}{2}k_{\lambda u}\tilde{\lambda}_u^2 + \frac{1}{2}k_{\lambda u}-\lambda_u^2 - \frac{2}{3}k_{\lambda u1}\tilde{\lambda}_u^{\frac{3}{2}}\\ & + \frac{4}{3}k_{\lambda u1}-\lambda_u^{\frac{3}{2}} - \frac{1}{2}k_{\lambda q}\tilde{\lambda}_q^2 + \frac{1}{2}k_{\lambda q}-\lambda_q^2 - \frac{2}{3}k_{\lambda q1}\tilde{\lambda}_q^{\frac{3}{2}}\\ & + \frac{4}{3}k_{\lambda q1}-\lambda_q^{\frac{3}{2}} - \frac{1}{2}k_{\lambda r}\tilde{\lambda}_r^2 + \frac{1}{2}k_{\lambda r}-\lambda_r^2 - \frac{2}{3}k_{\lambda r1}\tilde{\lambda}_r^{\frac{3}{2}}\\ & + \frac{4}{3}k_{\lambda r1}-\lambda_r^{\frac{3}{2}} - \frac{1}{2}k_{\hbar u}\tilde{h}_u^2 + \frac{1}{2}k_{\hbar u}\hbar_u^2 - \frac{2}{3}k_{\hbar u1}\tilde{h}_u^{\frac{3}{2}}\\ & + \frac{4}{3}k_{\hbar u1}\hbar_u^{\frac{3}{2}} - \frac{1}{2}k_{\hbar q}\tilde{h}_q^2 + \frac{1}{2}k_{\hbar q}\hbar_q^2 - \frac{2}{3}k_{\hbar q1}\tilde{h}_q^{\frac{3}{2}}\\ & + \frac{4}{3}k_{\hbar q1}\hbar_q^{\frac{3}{2}} - \frac{1}{2}k_{\hbar r}\tilde{h}_r^2 + \frac{1}{2}k_{\hbar r}\hbar_r^2 - \frac{2}{3}k_{\hbar r1}\tilde{h}_r^{\frac{3}{2}}\\ & + \frac{4}{3}k_{\hbar r1}\hbar_r^{\frac{3}{2}} + \frac{b_u}{2} + \frac{b_q}{2} + \frac{b_r}{2}\end{aligned} \tag{61}$$

Then, the following inequalities hold:

$$\dot{V} \le -\gamma_1 V - \gamma_2 V^{\frac{3}{4}} + \varsigma \tag{62}$$

where γ_1, γ_2 and ς satisfy the following:

$$\begin{aligned}&\gamma_1\\ &= \min\left\{k_\rho, k_\theta, k_\psi, k_u, k_q, k_r, (\kappa_u^{-1} - \frac{1}{2}), (\kappa_q^{-1} - \frac{1}{2}),\right.\\ &\quad \left.(\kappa_r^{-1} - \frac{1}{2}), \frac{k_{\lambda u}}{2}, \frac{k_{\lambda q}}{2}, \frac{k_{\lambda r}}{2}, \frac{k_{\hbar u}}{2}, \frac{k_{\hbar q}}{2}, \frac{k_{\hbar r}}{2}\right\}\end{aligned} \tag{63}$$

$$\begin{aligned}&\gamma_2\\ &= \min\left\{k_{\rho1}, k_{\theta1}, k_{\psi1}, k_{u1}, k_{q1}, k_{r1}, \kappa_{u1}, \kappa_{q1}, \kappa_{r1}, \frac{2}{3}k_{\lambda u1},\right.\\ &\quad \left.\frac{2}{3}k_{\lambda q1}, \frac{2}{3}k_{\lambda r1}, \frac{2}{3}k_{\hbar u1}, \frac{2}{3}k_{\hbar q1}, \frac{2}{3}k_{\hbar r1}\right\}\end{aligned} \tag{64}$$

$$\begin{aligned}&\varsigma\\ &= \frac{1}{2}B_u^2 + \frac{1}{2}B_q^2 + \frac{1}{2}B_r^2 + \frac{1}{2}k_{\lambda u}-\lambda_u^2 + \frac{4}{3}k_{\lambda u1}-\lambda_u^{\frac{3}{2}}\\ &\quad + \frac{1}{2}k_{\lambda q}-\lambda_q^2 + \frac{4}{3}k_{\lambda q1}-\lambda_q^{\frac{3}{2}} + \frac{1}{2}k_{\lambda r}-\lambda_r^2 + \frac{4}{3}k_{\lambda r1}-\lambda_r^{\frac{3}{2}}\\ &\quad + \frac{1}{2}k_{\hbar u}\hbar_u^2 + \frac{4}{3}k_{\hbar u1}\hbar_u^{\frac{3}{2}} + \frac{1}{2}k_{\hbar q}\hbar_q^2 + \frac{4}{3}k_{\hbar q1}\hbar_q^{\frac{3}{2}}\\ &\quad + \frac{1}{2}k_{\hbar r}\hbar_r^2 + \frac{4}{3}k_{\hbar r1}\hbar_r^{\frac{3}{2}} + \frac{b_u}{2} + \frac{b_q}{2} + \frac{b_r}{2}\end{aligned} \tag{65}$$

Hence, according to Lemma 1, all closed-loop system signals converge to a circular region $\Omega_V = \min\left\{\frac{\varsigma}{(1-\Theta)\gamma_1}, (\frac{\varsigma}{(1-\Theta)\gamma_2})^{\frac{3}{4}}\right\}$ near the origin in finite time.

$$\begin{aligned}T \le \max\Bigg\{&\frac{4}{\gamma_1\Theta}\ln(\frac{\gamma_1\Theta V^{\frac{1}{4}}(0)+\gamma_2}{\gamma_2}),\\ &\frac{4}{\gamma_1}\ln(\frac{\gamma_1\Theta V^{\frac{1}{4}}(0)+\gamma_2\Theta}{\gamma_2\Theta})\Bigg\}\end{aligned} \tag{66}$$

By choosing appropriate design parameters $k_\rho, k_\theta, k_\psi, k_u, k_q, k_r, \kappa_u, \kappa_q, \kappa_r, k_{\lambda u}, k_{\lambda q}, k_{\lambda r}, k_{\rho1}, k_{\theta1}, k_{\psi1}, k_{u1}, k_{q1}, k_{r1}, k_{\lambda u1}, k_{\lambda q1}$, and $k_{\lambda r1}$, Ω_V is limited to a small region $C^* = \min\left\{\frac{\varsigma}{(1-\Theta)\gamma_1}, (\frac{\varsigma}{(1-\Theta)\gamma_2})^{\frac{3}{4}}\right\}$. Then, one obtains:

$$\begin{aligned}&\frac{\beta_u^2}{\pi}\tan(\frac{\pi\rho_e^2}{2\beta_u^2}) + \frac{\beta_q^2}{\pi}\tan(\frac{\pi\theta_e^2}{2\beta_q^2}) + \frac{\beta_r^2}{\pi}\tan(\frac{\pi\psi_e^2}{2\beta_r^2})\\ &\quad + \frac{1}{2}u_e^2 + \frac{1}{2}q_e^2 + \frac{1}{2}r_e^2 + \frac{1}{2}u_{e1}^2 + \frac{1}{2}q_{e1}^2 + \frac{1}{2}r_{e1}^2\\ &\quad + \frac{1}{2}\tilde{\lambda}_u^2 + \frac{1}{2}\tilde{\lambda}_q^2 + \frac{1}{2}\tilde{\lambda}_r^2 + \frac{1}{2}\tilde{h}_u^2 + \frac{1}{2}\hbar_q^2 + \frac{1}{2}\tilde{h}_r^2 \le C^*\end{aligned} \tag{67}$$

which means that

$$\begin{aligned}&\frac{\beta_u^2}{\pi}\tan(\frac{\pi\rho_e^2}{2\beta_u^2}) \le C^*, \rho_e^2 \le \frac{2\beta_u^2}{\pi}\tan^{-1}(\frac{\pi C^*}{\beta_u^2}) < \beta_u^2\\ &\frac{\beta_q^2}{\pi}\tan(\frac{\pi\theta_e^2}{2\beta_q^2}) \le C^*, \theta_e^2 \le \frac{2\beta_q^2}{\pi}\tan^{-1}(\frac{\pi C^*}{\beta_q^2}) < \beta_q^2\\ &\frac{\beta_r^2}{\pi}\tan(\frac{\pi\psi_e^2}{2\beta_r^2}) \le C^*, \psi_e^2 \le \frac{2\beta_r^2}{\pi}\tan^{-1}(\frac{\pi C^*}{\beta_r^2}) < \beta_r^2\end{aligned} \tag{68}$$

From (67) and (68), the following inequalities hold:

$$\begin{aligned}&|\rho_e| < |\beta_u|, |\theta_e| < |\beta_q|, |\psi_e| < |\beta_r|, |u_e| < \sqrt{2C^*},\\ &|q_e| < \sqrt{2C^*}|r_e| < \sqrt{2C^*}, |u_{e1}| < \sqrt{2C^*}, |q_{e1}| < \sqrt{2C^*},\\ &|r_{e1}| < \sqrt{2C^*}, |\tilde{\lambda}_u| < \sqrt{2C^*}|\tilde{\lambda}_q| < \sqrt{2C^*},\\ &|\tilde{\lambda}_r| < \sqrt{2C^*}, |\tilde{h}_u| < \sqrt{2C^*}, |\tilde{h}_q| < \sqrt{2C^*}, |\tilde{h}_r| < \sqrt{2C^*}\end{aligned} \tag{69}$$

In conclusion, the errors $\rho_e, \theta_e, \psi_e, u_e, q_e, r_e, u_{e1}, q_{e1}, r_{e1}, \tilde{\lambda}_u, \tilde{\lambda}_q, \tilde{\lambda}_r, \tilde{h}_u, \tilde{h}_q, \tilde{h}_r$ are practical finite-time stable, and the proof is complete.

Remark 7: According to equations (63) and (64), one can obtain that when the design parameters $k_\rho, k_\theta, k_\psi, k_u, k_q, k_r, k_{\lambda u}, k_{\lambda q}, k_{\lambda r}, k_{\rho1}, k_{\theta1}, k_{\psi1}, k_{u1}, k_{q1}, k_{r1}, k_{\lambda u1}, k_{\lambda q1}$,and $k_{\lambda r1}$ increase, the parameters $\kappa_u, \kappa_q, \kappa_r, \kappa_{u1}, \kappa_{q1}$,and κ_{r1}, decrease, and γ_1, and $\gamma_2$increase, thus changing the convergence time of the controller and steady state errors. Therefore, appropriate parameters can be selected to obtain better control performance.

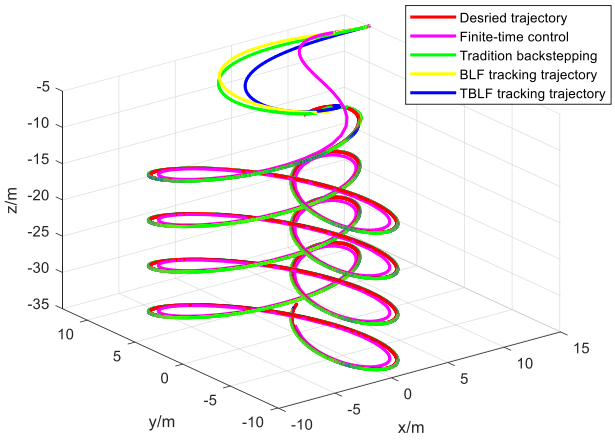

FIGURE 3. Trajectory tracking.

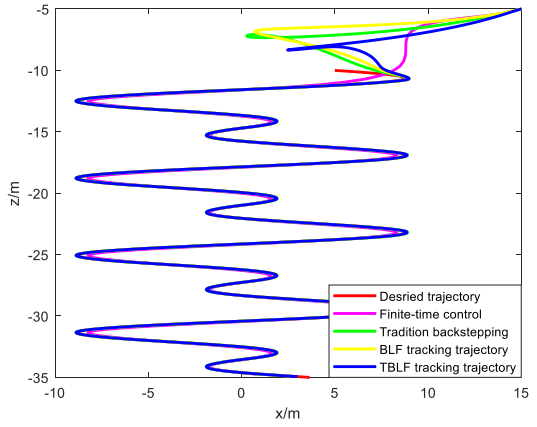

FIGURE 4. XZ plot.

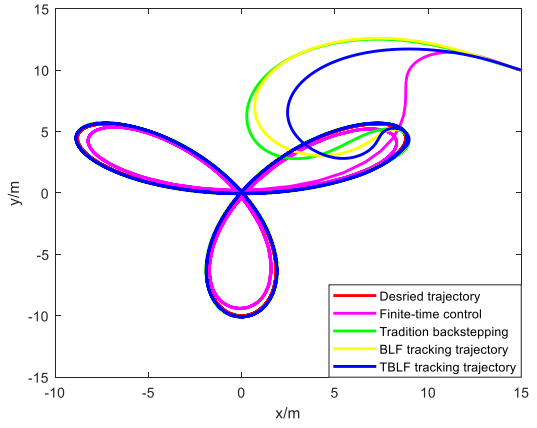

FIGURE 5. XY plot.

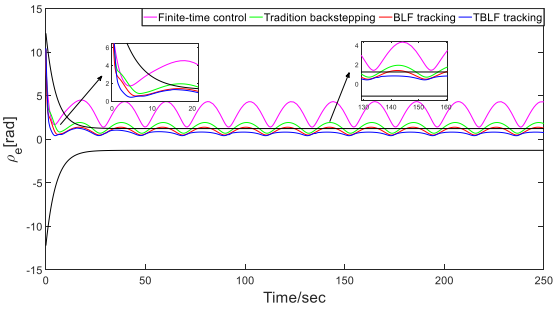

FIGURE 6. Tracking error ρ_e.

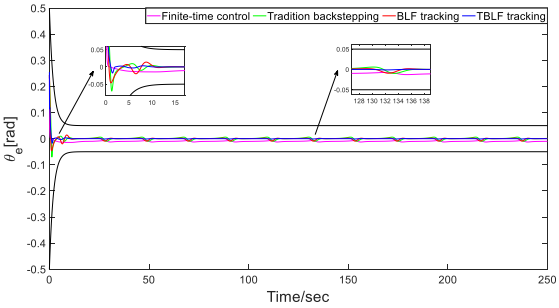

FIGURE 7. Tracking error θ_e.

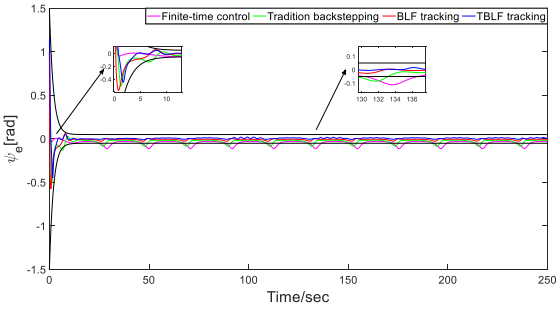

FIGURE 8. Tracking error ψ_e.

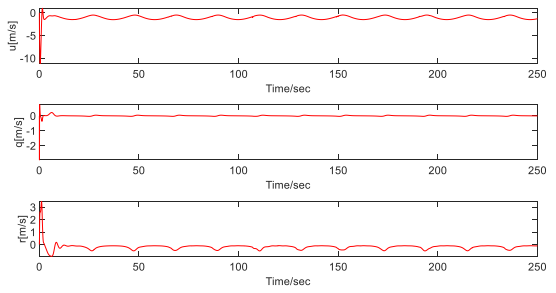

FIGURE 9. Velocities.

III. SIMULATION RESULTS

In order to verify that the proposed control scheme is effective, simulation results of the developed controller in this paper are compared with the finite-time control strategy, the existing literature [22] and the traditional backstepping control scheme under the same simulation situation [7]: $m_{11} = 25kg, m_{22} = 17.5kg, m_{33} = 30kg, m_{55} = 22.5kg \cdot m^2, m_{66} = 15kg \cdot m^2, d_{11} = 30kg \cdot s^{-1}, d_{22} = 30kg \cdot s^{-1}, d_{33} = 30kg \cdot s^{-1}, d_{55} = 20kg \cdot s^{-1}, d_{66} = 20kg \cdot s^{-1}, \rho g\overline{GM}_L = 5.$

The reference trajectory should be set as:$x_d = 5\sin 0.2t + 5\cos 0.1t, y_d = 5\sin 0.1t + 5\cos 0.2t, z_d = -10 - 0.1t.$ We use the following gains for simulation:$k_\rho = 0.1, k_\theta = 8.6, k_\psi = 2.8, k_u = 2, k_q = 5, k_r = 8, k_{\rho 1} = k_{\theta 1} = k_{\psi 1} =$

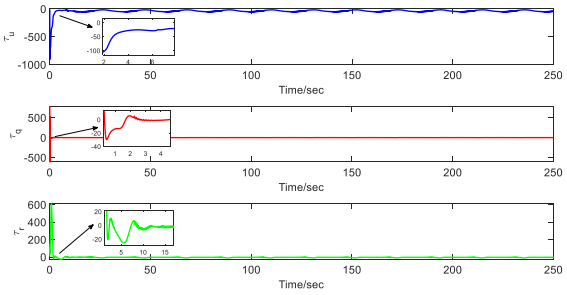

FIGURE 10. Actual control inputs.

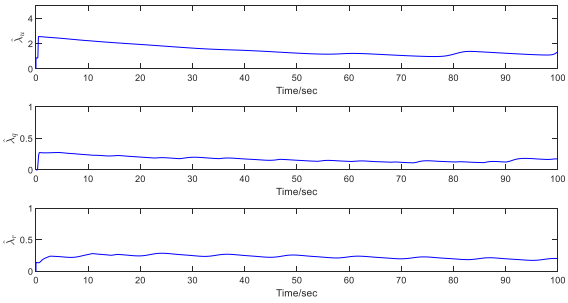

FIGURE 11. Adaptive parameters.

0.01, $k_{\partial 1} = 0.1$, κ_∂=0.01, and $k_{\bar{\lambda}\partial}$=0.01, where $\partial = u, q, r$. The performance functions in (8) are specified as:$\beta_u = (11 - 0.05)\exp(-0.3t) + 1.25$, $\beta_q = (\pi/6 - 0.05)\exp(-0.5t) + 0.05$, $\beta_r = (\pi/2 - 0.05)\exp(-0.5t) + 0.05$. We use the following signals as ocean environment disturbances $\tau_k = 0.5sign(k) + 0.5\sin(t/10), k = u, v, w, q, r$. The initial state of the AUV is given by $x(0) = 15, y(0) = 10, z(0) = -5, \theta(0) = -\pi/10, \psi(0) = -\pi/7, u(0) = 0, v(0) = 0, w(0) = 0, q(0) = 0, r(0) = 0$.

Simulation results are illustrated in Figs.3-11. Figs.3-5 show the trajectory tracking result, which indicates that the AUV can successfully track the target. Figs.6-8 shows tracking errors and the prescribed performance constraints. Compared with the tradition backstepping method and BLF tracking trajectory method, the proposed controller converges quickly and has better control precision. Fig.9 shows the velocities of the AUV in u, q and r. Fig.10 illustrates that the three controllable inputs τ_u, τ_q and $\tau_r$are continuous and smooth. Fig.11 shows the adaptive parameters $\hat{\bar{\lambda}}_u$, $\hat{\bar{\lambda}}_q$ and $\hat{\bar{\lambda}}_r$.

IV. CONCLUSION

In this paper, a finite-time convergent control strategy based on the tan-type barrier Lyapunov function backstepping method, combining DSC technique and MLP algorithm, is proposed for the trajectory tracking problem of an underactuated autonomous underwater vehicle. The proposed controller ensures that all signals of the closed-loop system are bounded, and the AUV can converge to the desired trajectory in a finite time. The DSC technique improves the efficiency of the controller by simplifying the calculation process, while the MLP also enhances the robustness against the model uncertainties. Then, an adaptive law can effectively estimate NN errors and environmental disturbances to guarantee the accuracy of system. Finally, simulation results show that the proposed controller is effective.

REFERENCES

[1] W. Shi, S. Song, C. Wu, and C. L. P. Chen, "Multi pseudo Q-learning-based deterministic policy gradient for tracking control of autonomous underwater vehicles," *IEEE Trans. Neural Netw. Learn. Syst.*, vol. 30, no. 12, pp. 3534–3546, Dec. 2019.

[2] L. Lapierre and D. Soetanto, "Nonlinear path-following control of an AUV," *Ocean Eng.*, vol. 34, nos. 11–12, pp. 1734–1744, 2007.

[3] C. T. Bandara, L. N. Kumari, S. Maithripala, and A. Ratnaweera, "Vehicle-fixed-frame adaptive controller and intrinsic nonlinear PID controller for attitude stabilization of a complex-shaped underwater vehicle," *J. Mechtron. Robot.*, vol. 4, no. 1, pp. 254–264, Jan. 2020.

[4] Z. Peng, D. Wang, and J. Wang, "Containment control of networked autonomous underwater vehicles guided by multiple leaders using predictor-based neural DSC approach," in *Proc. 5th Int. Conf. Intell. Control Inf. Process.*, Aug. 2014, pp. 360–365.

[5] F. Rezazadegan, K. Shojaei, F. Sheikholeslam, and A. Chatraei, "A novel approach to 6-DOF adaptive trajectory tracking control of an AUV in the presence of parameter uncertainties," *Ocean Eng.*, vol. 107, pp. 246–258, Oct. 2015.

[6] L. Qiao and W. Zhang, "Double-loop integral terminal sliding mode tracking control for UUVs with adaptive dynamic compensation of uncertainties and disturbances," *IEEE J. Ocean. Eng.*, vol. 44, no. 1, pp. 29–53, Jan. 2019.

[7] K. Shojaei and M. Dolatshahi, "Line-of-sight target tracking control of underactuated autonomous underwater vehicles," *Ocean Eng.*, vol. 133, pp. 244–252, Mar. 2017.

[8] B. S. Park, "Neural network-based tracking control of underactuated autonomous underwater vehicles with model uncertainties," *J. Dyn. Syst., Meas., Control*, vol. 137, no. 2, Feb. 2015, Art. no. 021004.

[9] T. Elmokadem, M. Zribi, and K. Youcef-Toumi, "Terminal sliding mode control for the trajectory tracking of underactuated autonomous underwater vehicles," *Ocean Eng.*, vol. 129, pp. 613–625, Jan. 2016.

[10] Y. Yan and S. Yu, "Sliding mode tracking control of autonomous underwater vehicles with the effect of quantization," *Ocean Eng.*, vol. 151, pp. 322–328, Mar. 2018.

[11] Z. Yan, M. Wang, and J. Xu, "Robust adaptive sliding mode control of underactuated autonomous underwater vehicles with uncertain dynamics," *Ocean Eng.*, vol. 173, pp. 802–809, Feb. 2019.

[12] M. Chen and D. Zhu, "Multi-AUV cooperative hunting control with improved Glasius bio-inspired neural network," *J. Navigat.*, vol. 72, no. 3, pp. 759–776, May 2018.

[13] J. Wang, C. Wang, Y. Wei, and C. Zhang, "Command filter based adaptive neural trajectory tracking control of an underactuated underwater vehicle in three-dimensional space," *Ocean Eng.*, vol. 180, pp. 175–186, May 2019.

[14] X. Guo, W. Yan, and R. Cui, "Neural network-based nonlinear sliding-mode control for an AUV without velocity measurements," *Int. J. Control*, vol. 92, no. 3, pp. 677–692, 2020.

[15] O. Elhaki and K. Shojaei, "Neural network-based target tracking control of underactuated autonomous underwater vehicles with a prescribed performance," *Ocean Eng.*, vol. 167, pp. 239–256, Nov. 2018.

[16] B. Miao, T. Li, and W. Luo, "A DSC and MLP based robust adaptive NN tracking control for underwater vehicle," *Neurocomputing*, vol. 111, pp. 184–189, Jul. 2013.

[17] C. Liu, X. Liu, H. Wang, Y. Zhou, and S. Lu, "Finite-time adaptive tracking control for unknown nonlinear systems with a novel barrier Lyapunov function," *Inf. Sci.*, vol. 528, pp. 231–245, Aug. 2020.

[18] G. Zhang, Y. Deng, and W. Zhang, "Robust neural path-following control for underactuated ships with the DVS obstacles avoidance guidance," *Ocean Eng.*, vol. 143, pp. 198–208, Oct. 2017.

[19] G. Zhang, C. Huang, X. Zhang, and W. Zhang, "Practical constrained dynamic positioning control for uncertain ship through the minimal learning parameter technique," *IET Control Theory Appl.*, vol. 12, no. 18, pp. 2526–2533, 2018.

[20] K. Mei and S. Ding, "HOSM controller design with asymmetric output constraints," *Sci. China Inf. Sci.*, vol. 65, no. 8, pp. 1–2, 2022.

[21] K. Mei, S. Ding, and C.-C. Chen, "Fixed-time stabilization for a class of output-constrained nonlinear systems," *IEEE Trans. Syst., Man, Cybern. Syst.*, early access, Feb. 8, 2022, doi: 10.1109/TSMC.2022.3146011.
[22] Z. Zheng, L. Ruan, and M. Zhu, "Output-constrained tracking control of an underactuated autonomous underwater vehicle with uncertainties," *Ocean Eng.*, vol. 175, pp. 241–250, Dec. 2019.
[23] Y.-J. Liu and S. Tong, "Barrier Lyapunov functions-based adaptive control for a class of nonlinear pure-feedback systems with full state constraints," *Automatica*, vol. 64, pp. 70–75, Feb. 2016.
[24] T. Xie, Y. Li, Y. Jiang, L. An, and H. Wu, "Backstepping active disturbance rejection control for trajectory tracking of underactuated autonomous underwater vehicles with position error constraint," *Int. J. Adv. Robot. Syst.*, vol. 17, no. 2, pp. 1–12, 2020.
[25] J. Zhou, X. Zhao, T. Chen, Z. Yan, and Z. Yang, "Trajectory tracking control of an underactuated AUV based on backstepping sliding mode with state prediction," *IEEE Access*, vol. 7, pp. 181983–181993, 2019.
[26] Z. Yan, Z. Yang, J. Zhang, J. Zhou, A. Jiang, and X. Du, "Trajectory tracking control of UUV based on backstepping sliding mode with fuzzy switching gain in diving plane," *IEEE Access*, vol. 7, pp. 166788–166795, 2019.
[27] J. Guerrero, J. Torres, V. Creuze, and A. Chemori, "Trajectory tracking for autonomous underwater vehicle: An adaptive approach," *Ocean Eng.*, vol. 172, no. 2, pp. 511–522, Jan. 2019.
[28] K. D. Do and J. Pan, *Control of Ships and Underwater Vehicles: Design for Underactuated and Nonlinear Marine Systems*. London, U.K.: Springer, 2009.
[29] T. I. Fossen, "Marine control systems-guidance. Navigation, and control of ships, rigs and underwater vehicles," *Mar. Cybern.*, 2002.
[30] C. P. Bechlioulis and G. A. Rovithakis, "Robust adaptive control of feedback linearizable MIMO nonlinear systems with prescribed performance," *IEEE Trans. Autom. Control*, vol. 53, no. 9, pp. 2090–2099, Oct. 2008.
[31] M. Chen, S. S. Ge, and B. Ren, "Adaptive tracking control of uncertain MIMO nonlinear systems with input constraints," *Automatica*, vol. 47, no. 3, pp. 452–465, Mar. 2011.
[32] J. Yu, P. Shi, and L. Zhao, "Finite-time command filtered backstepping control for a class of nonlinear systems," *Automatica*, vol. 92, pp. 173–180, Jun. 2018.
[33] J. Ni, Z. Wu, L. Liu, and C. Liu, "Fixed-time adaptive neural network control for nonstrict-feedback nonlinear systems with deadzone and output constraint," *ISA Trans.*, vol. 97, pp. 458–473, Feb. 2020.
[34] X. Jin, "Adaptive finite-time fault-tolerant tracking control for a class of MIMO nonlinear systems with output constraints," *Int. J. Robust Nonlinear Control*, vol. 27, no. 5, pp. 722–741, Mar. 2017.
[35] S. He, C. Dong, and S.-L. Dai, "Adaptive neural formation control for underactuated unmanned surface vehicles with collision and connectivity constraints," *Ocean Eng.*, vol. 226, Apr. 2021, Art. no. 108834, doi: 10.1016/j.oceaneng.2021.108834.

HAITAO LIU (Member, IEEE) received the Ph.D. degree from the School of Mechanical & Automotive Engineering, South China University of Technology, Guangzhou, China, in 2012. He is currently a Professor with the School of Mechanical and Power Engineering, Guangdong Ocean University, Zhanjiang, China. His research interests include theory and applications of nonlinear control, and robotics.

BINGXIN MENG received the B.E. degree from Shenyang Jianzhu University, Shenyang, China, in 2019. He is currently pursuing the master's degree with the School of Mechanical and Power Engineering, Guangdong Ocean University. His research interests include underactuated autonomous underwater vehicles and robust adaptive control.

XUEHONG TIAN received the M.E. degree in mechanical engineering from Guangdong Ocean University, Zhanjiang, China, in 2018. She is currently an Associate Professor with the School of Mechanical and Power Engineering, Guangdong Ocean University. Her research interests include robot control, multi-agent systems, and nonlinear systems design.